J Control Autom Electr Syst (2013) 24:324–338
DOI 10.1007/s40313-013-0017-2

Probabilistic Algorithms for Power Load Flow and Short-Circuit Analysis in Distribution Networks with Dispersed Generation

César Augusto Peñuela Meneses · Mauricio Granada Echeverri · Jose R. Sanches Mantovani

Received: 31 October 2011 / Revised: 21 March 2012 / Accepted: 22 May 2012 / Published online: 3 April 2013

Abstract In this paper, an approach for probabilistic analysis of unbalanced three-phase weakly meshed distribution systems with dispersed generation is presented. The approach considers uncertainty in both load demand and the injected power of dispersed generators. In order to achieve high computational efficiency, the approach makes use of both an efficient method for probabilistic analysis and a radial power flow. The probabilistic strategy used is the well-known Three-Point Estimate Method. In the other hand, classical models based on the sequence impedance are implemented for modeling synchronous machines, asynchronous machines, and electronically interfaced sources. These models aim to consider the impact on the power flows from the installation of dispersed generators. A small-size test system, as well as the modified IEEE 123 bus system, is used to show the operation and effectiveness of the proposed approach. A Monte Carlo Simulations method is used to validate the results.

Keywords Distributed generation · Distribution power flow · Short-circuit analysis · Probabilistic analysis · Point Estimate Method

C. A. Peñuela Meneses (✉) · J. R. Sanches Mantovani
Laboratório de Planejamento de Energia Elétrica, Departamento de Engenharia Elétrica, Universidade Estadual Paulista - Campus de Ilha Solteira, Ilha Solteira, SP, Brazil
e-mail: cesar_penuela@hotmail.com;
capenuela@unilibrepereira.edu.co

J. R. Sanches Mantovani
e-mail: mant@dee.feis.unesp.br

M. G. Echeverri
Programa de ingeniería eléctrica, Grupo de planeamiento eléctrico, Universidad Tecnológica de Pereira, Pereira, Risaralda, Colombia
e-mail: granadam@ieee.org

1 Introduction

For the past few years a lot has been discussed about the real advantages of dispersed generation (DG) in distribution networks (Pepermans et al. 2001; Zhu and Tomosovic 2002). Some significant advantages involve power-loss reduction, increasing reliability, and improving voltage profiles. However, the loss of selectivity in the protection system, and the increase in short-circuit currents, appears as problems arising from the installation of DGs (Brahma and Adly 2004). To identify these issues, and to proceed to resolve them, an efficient and robust computational tool for analysis and planning distribution networks with DG is required.

The traditional tools for calculating the load flows are useful to determine the operating point of any electrical system. However, these tools consider a deterministic behavior in several electrical parameters, such as the load demand and the power generation. In fact, the above are influenced by external conditions with difficult prediction, such as the climate and the customer demand. To consider the real impact on the power system from parameters with uncertain behavior, a probabilistic approach must be considered. Thus, the real state of the energy system could be made on the basis of the diagnosis of variables with an estimated probability of occurrence. Due to the large uncertain behavior of several of distributed generation sources, especially those based on renewable primary energy, the need of developing specialized computational tools for the simulation of electrical systems is justified.

There are several strategies proposed in the academic research for the analysis of probabilistic load flow, where the deterministic calculation of state variables is done through the Newton-Raphson algorithm (Chun-Lien 2010). In distribution systems, it is widely advantageous to employ numerical techniques that allow taking advantage of the distribution

systems' radial topology feature. These techniques are well-known as backward/forward algorithms (Shirmohammadi et al. 1988). To consider distribution systems with multiple sources and to perform short-circuit analyses (Zhang et al. 1995), the compensation theory could be applied (Tinney 1972).

At any electrical network, the intensity of the short-circuit current depends on the operating point of the electrical system at the time of the fault, the fault location, and the impedance existing between the conductive element and the ground surface. Thus, in addition to the uncertain variables existing in the pre-fault condition, it is necessary to consider the value of the contact impedance at the fault point. This fact has been addressed less frequently in the academic literature, and the methodology is always based on Monte Carlo simulations (Bordalo et al. 2006).

On the other hand, several studies on the literature consider the operation of distributed generation as a negative load model. However, if a more detailed analysis is required, the behavior of distributed generation and its impact on the distribution network must be reflected. To accomplish this, it is necessary to consider the internal parameters of DGs. Nevertheless, the determination of a mathematical model of DGs is a complex task because their parameters are governed by time-varying inductive couplings—in the case of rotating machines (Anderson 1998)—or filtering devices and instantaneous control of switching elements—in the case of sources with power electronic interface (Balaguer et al. 2011). In order to contour this problem, the models for DGs are normally based on equivalent circuits of zero, positive, and negative sequences. This strategy has showed satisfactory results when applied to the solution of electrical systems in the steady-state (Abdel-Akher et al. 2005; Chen et al. 1990; Zakaria Kamh and Iravani 2010). To accomplish this transformation, it is assumed the possibility of decomposing the whole distribution network in sequence components. Although, the aforementioned fact cannot always be directly applied due to the unbalance behavior typically found in the untransposed lines of the distribution systems, or by the presence of single-phase circuits.

Recently, the probabilistic analysis of uncertain variables in power flow algorithms has been widely addressed through approximated estimation methods (Gallego et al. 2012; Granada et al. 2010; Hong 1998), rather than the traditional Monte Carlo Simulation Method (Rubinstein 1981). This latter is particularly complex and more robust, though, it requires greater computational effort. For this reason its use in planning studies is hindered. Instead, Chun-Lien (2005) uses the Two-Point Estimate Method to calculate the power flow in transmission systems with uncertainties in load demand, power generation, and the parameters of lines. Chun-Lien (2010) applied the same procedure to for analyzing distribution systems with distributed generation penetration, assuming a single-phase system modeling, and considering the DGs as a negative load connected to the grid. Using the above DG modeling, in addition to the Three-Point Estimate Method, Morales et al. (2010) analyzes the impact in the distribution systems when wind power generation is connected, and its high dependence with the wind speed is discussed. Neither of these papers considers the interaction between GDs and the grid when the operation is turning unbalanced.

In this paper, two algorithms to calculate the load flow and short-circuit currents are proposed. Both algorithms use an efficient probabilistic analysis of the distribution system with DGs and uncertain variables. The random variables are analyzed using the technique of Three-Point Estimate Method (Hong 1998). The pre-fault operation point is determined by a deterministic load flow based on the backward/forward algorithm. In addition, the phase frame is used to represent the steady-state variables. The DGs are modeled in accordance with the technology used for power generation, considering that power exchanged can be controlled to maintain voltage level and the active power (PV bus), the power factor (PQ bus), or only with monitoring of the active power (P bus). In each case, the models are determined with the basis of knowledge of the parameters of the zero, positive and negative sequences of the generator. The post-fault state is calculated by applying a special case of the compensation methodology to analyze short-circuit currents in the phase frame, as described in (Zhang et al. 1995). In addition to the algorithm presented by Zhang et al. (1995), the proposed algorithm (PA) in this paper considers the effects of the contact impedance with the ground and, focuses on the contribution of distributed generation sources in the short-circuit current, which depends on the dynamic behavior of each type of distributed generation technology after the fault condition. The assumption of the existence of the fault impedance and the contribution of DG can improve the coordination of protective devices, as the values of currents to trip the protective devices for faults within their protection zones could be estimated.

In addition to this introductory section, this paper includes the following sections: a Sect. 2 presents a mathematical modeling for DGs in accordance with the technology used for the processing of the primary source, as well as the coupling of DGs to the grid. Sections 3 and 4 present the most relevant insights of deterministic algorithms for the calculation of load flow and short-circuit, respectively. In Sect. 5, in turn, the aspects involved in probabilistic analysis of random variables in the Three-Point Estimate Method are examined. Finally, the Sect. 6 discusses the results of simulations of computational implementation. An eleven bus test system and a modified IEEE 123 bus test system are used to show the advantage of the proposed methodology.

2 Dispersed Generation Modeling

The generator is the component that aims to convert energy from the primary source into electrical energy. In this process electrical machines are used most frequently, i.e., the direct current generator, and the synchronous and asynchronous generator. However, other operations could be used. For example, chemical or physical processes are implemented in fuel cells, and photovoltaic cells, respectively. In such cases, the electricity generated must be processed in electronic-based circuits before the injection into the grid. Thus, due to the existence of different devices with different operating modes, it is concluded that a mathematical model to simulate the effects caused in electrical systems is required when such devices are connected to the distribution network. In the present section of the paper, the models used for each type of distributed generator are described.

2.1 Synchronous Generator

The determination of the mathematical model for rotating machines is a complex problem. This is because their impedances are governed by inductive coupling which varies with the relative positioning of the magnetic structures. In load flow studies, it is sufficient to implement a simplified mathematical model based on the reactance of zero-sequence, X_0, positive-sequence, X_1, and negative-sequence, X_2. These parameters are widely used in unbalanced power system analyses (Anderson 1998). The circuit model used for the synchronous generator is illustrated in Fig. 1.

In Fig. 1, Z_{GD} is the phase impedance matrix of the generator. It is calculated using the symmetrical components transformation matrix (Anderson 1998), as described in (1). The resistive components of windings are omitted due to the typically low R/X relation. In (1), a is the operator with unitary magnitude and phase of 120^o.

$$[\mathbf{Z_{GD}}] = \frac{1}{3}\begin{bmatrix} 1 & 1 & 1 \\ 1 & a & a^2 \\ 1 & a^2 & a \end{bmatrix}\begin{bmatrix} X_0 & 0 & 0 \\ 0 & X_1 & 0 \\ 0 & 0 & X_2 \end{bmatrix}\begin{bmatrix} 1 & 1 & 1 \\ 1 & a^2 & a \\ 1 & a & a^2 \end{bmatrix} \quad (1)$$

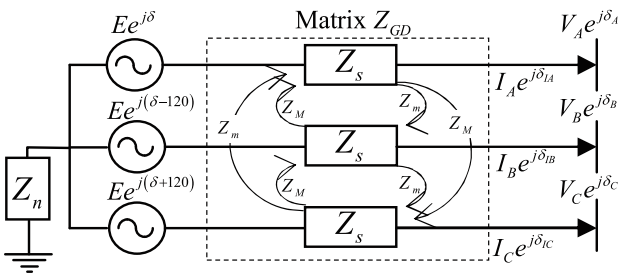

Fig. 1 Mathematical modeling for synchronous generators

2.2 Asynchronous Generator

The analyses of asynchronous machines may be performed using the approximate model shown in Fig. 2, where s is the slip of the machine, R_s and X_s are respectively the resistance and reactance of the equivalent field winding, X_m is the reactance of magnetization, and, R_r and X_r are the resistance and reactance of the rotor field winding referenced to the stator, respectively (Anderson 1998).

This model is appropriate in balanced operation conditions. Therefore, to consider the nature of unbalanced electrical distribution systems, the negative-sequence circuit must be added, as shown in Fig. 3. It is noteworthy that the internal connection of asynchronous machines generally contains no ground connection. This condition makes it unnecessary to analyze the zero sequence quantities.

In Figs. 2 and 3, the dependence of machine operation with the slip s is evident. In this paper, the strategy adopted to simulate the operation of the generator is to assume a continuous control of the slip. That allows the control of the active power supplied by the source within its permitted bounds. Moreover, the reactive power absorbed by the machine is calculated as a function of the voltage at its terminals, the circuital parameters, and the slip. According to this model, the calculation of the current supplied by the asynchronous generator can be made through the following algorithm:

i. For k-th iteration of the load flow algorithm, transform the voltage level at the terminals of the generator to the symmetrical components:

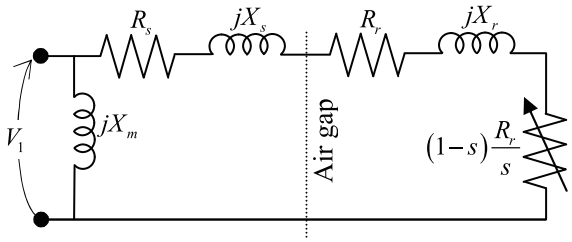

Fig. 2 Equivalent circuit of positive sequence for asynchronous generator

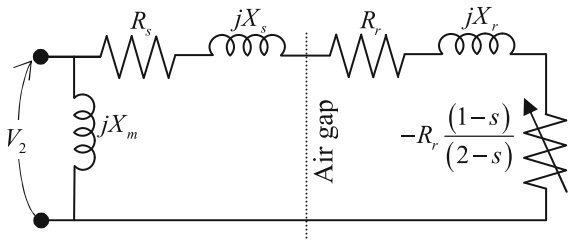

Fig. 3 Negative-sequence circuit for asyncrhonous generators

$$\begin{bmatrix} V_0 \\ V_1 \\ V_2 \end{bmatrix} = \frac{1}{3} \begin{bmatrix} 1 & 1 & 1 \\ 1 & a & a^2 \\ 1 & a^2 & a \end{bmatrix} \begin{bmatrix} V_a \\ V_b \\ V_c \end{bmatrix} \tag{2}$$

ii. With the value of the voltage magnitude in the positive sequence circuit, V_{1m}, apply the Eq. (3) to calculate the value of the slip s. This value must allow a scheduled injection power P_{sh}. In this case, it should be noted that $P_{sh} < 0$, because the asynchronous generator has a load notation.

$$s = \frac{R_s}{R - R_r} \tag{3}$$

where:

$$R = \frac{(V_{1m})^2 + \sqrt{(V_{1m})^4 - (2 \cdot P_{sh} \cdot (X_s + X_r))^2}}{2 \cdot P_{sh}} \tag{4}$$

iii. With the aid of the Eq. (5), calculate the current in the positive-sequence circuit:

$$I_1 = \frac{V_1}{R + j\,(X_s + X_r)} + \frac{V_1}{jX_m} \tag{5}$$

iv Using the Eq. (6), determine the current in the negative-sequence circuit. At this step, the value of the slip calculated in step *ii* is considered.

$$I_2 = \frac{V_2}{\left(R_s + \frac{R_r}{2-s}\right) + j\,(X_s + X_r)} + \frac{V_2}{jX_m} \tag{6}$$

v Transform the sequence currents obtained in the steps *iii* and *iv* to the phase components frame. To do this, the Eq. (7) is used, in which the zero-sequence current is set to null.

$$\begin{bmatrix} I_a \\ I_b \\ I_c \end{bmatrix} = \begin{bmatrix} 1 & 1 & 1 \\ 1 & a^2 & a \\ 1 & a & a^2 \end{bmatrix} \begin{bmatrix} 0 \\ I_1 \\ I_2 \end{bmatrix} \tag{7}$$

2.3 Electronically Interfaced Units

In this paper, DG with voltage source controller (VSC) is modeled as proposed by Zakaria Kamh and Iravani (2010). In such case is assumed that the generator has a power storage system which allows a controlled exchange of power energy, even with variability in the primary energy source. Hence, the model showed in Fig. 1 can still be used when electronically interfaced DG units are considered. To do this, the parameters listed in Eqs. (8) and (9) must be applied.

$$Z_0 = 0 \tag{8}$$

$$Z_1 = Z_2 = R_f + jX_f \tag{9}$$

where R_f and X_f are the equivalent impedance of both the coupling transformer and the filtering system. The latter is used to reduce penetration of harmonic currents into the grid (Kosterev 1997).

3 Load Flow Algorithm

In this paper, the compensation-based radial power flow is used to determine the operation point of the system (Cheng and Shirmohammadi 1995). This methodology has been chosen due to its computational efficiency when applied to weakly meshed networks. Such feature can be exploited in distribution systems, in which the radial topology is a prevalent condition. Furthermore, the methodology is robust enough to consider voltage-controlled DG connected to the grid. The algorithm is basically shared in three steps: branch current calculations, voltage updating, and estimation of breakpoint currents. The following presents a brief description of these steps.

3.1 Branch Current Calculation

This step is known as the backward sweep operation and is executed at each iteration k of the algorithm. The objective is to estimate the branch currents at the whole system by mean of the *first Kirchhoff law* application. The process starts at the farthest nodes from the substation and applies the Eq. (10) to determine the current flowing at each branch of the distribution system.

$$\begin{bmatrix} J_{ia}^k \\ J_{ib}^k \\ J_{ic}^k \end{bmatrix} = -\begin{bmatrix} I_{ia}^k \\ I_{ib}^k \\ I_{ic}^k \end{bmatrix} + \sum_{m \in M} \begin{bmatrix} J_{ma}^k \\ J_{mb}^k \\ J_{mc}^k \end{bmatrix} \tag{10}$$

In the Eq. (10), $J_{(ia,b,c)}^k$ are the three-phase currents at the branch linking the buses i and m. In this case, the bus m is closest to the substation than the bus i, and the set M contains all the tie-lines with the bus i. Furthermore, $I_{(ia,b,c)}^k$ corresponds to the three-phase currents injected by the dispersed generators connected at bus i. It must be noted that the line modeling for distribution system is assumed as the standard π-model with concentrated parameters (Cheng and Shirmohammadi 1995).

3.2 Voltage Updating

This step is known as the forward sweep and applies the *Second Kirchhoff law* to determine the voltage profile at the buses of the distribution system. The process begins at the substation and employs Eq. (11) to asses the voltage level at the bus i when the three-phase currents J_{ia}, J_{ib}, and J_{ic}

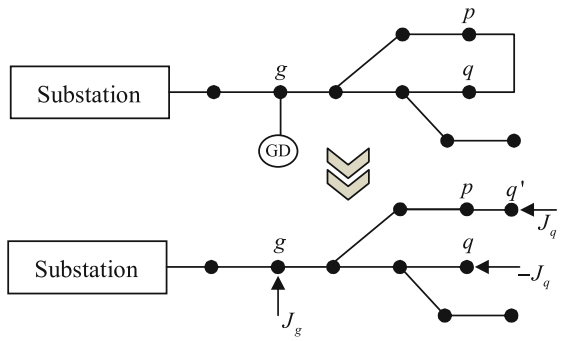

Fig. 4 Breakpoint currents selection and radial topology generation

flow in the branch linking the buses i and j. In this case, bus j is closest to the substation than bus i.

$$\begin{bmatrix} V_{ia}^k \\ V_{ib}^k \\ V_{ic}^k \end{bmatrix} = \begin{bmatrix} V_{ja}^k \\ V_{jb}^k \\ V_{jc}^k \end{bmatrix} + \begin{bmatrix} Z_{aa} & Z_{ab} & Z_{ac} \\ Z_{ba} & Z_{bb} & Z_{bc} \\ Z_{ca} & Z_{cb} & Z_{cc} \end{bmatrix} \begin{bmatrix} J_{ia} \\ J_{ib} \\ J_{ic} \end{bmatrix} \tag{11}$$

It must be noted that, in this paper, the parameters of the line, as well as transformers and switch, has 3×3-dimension. In order to accomplish this, the modeling of series elements into the backward/forward algorithm presented by Baran and Staton (1997) is used.

3.3 Estimation of Breakpoint Currents

The compensation theory used in this paper is originally introduced by Tinney (1972). The strategy is essentially used to consider meshed circuits in distribution systems, such as that produced by dispersed generators, section loops, or short-circuit faults. To implement the radial power-flow algorithm, the meshed circuits must be represented by equivalent circuits with radial topology. This process is graphically shown in Fig. 4. In addition, only one DG and one circuit loop are considered to preserve simplicity. However, for the sake of generality, the strategy could be extended to several breakpoints. It is easy to observe that circuit loops and voltage-controlled DGs are replaced by current sources J_q and J_g, respectively. These sources are named as breakpoint injected currents. It is also noted that one fictitious bus is created when circuit loops are treated.

Hence, for the k-th iteration of the algorithm, the Eq. (12) is implemented to determine the three-phase current injected at the breakpoints.

$$\left[\mathbf{J}_{g,q^k}\right] = \left[\mathbf{J}_{g,q^{k-1}}\right] + \left[\Delta\mathbf{J}_{g,q}^k\right] \tag{12}$$

In (12), $\Delta\mathbf{J}_{g,q^k}$ is the increasing vector of the breakpoint currents, which can be estimated with Eq. (13).

$$\begin{bmatrix} \mathbf{Z}_g & \mathbf{Z}_{gq} \\ \mathbf{Z}_{gq} & \mathbf{Z}_q \end{bmatrix} \begin{bmatrix} \Delta\mathbf{J}_g^k \\ \Delta\mathbf{J}_q^k \end{bmatrix} = \begin{bmatrix} \mathbf{E}_{g^k} - \mathbf{E}_g \\ \mathbf{V}_{q'}^k - \mathbf{V}_q^k \end{bmatrix} \tag{13}$$

Equation (13) in turn, could be rewritten as shown in Eq. (14).

$$[\mathbf{Z}]\left[\Delta\mathbf{J}_{g,q}^k\right] = \left[\Delta\mathbf{V}_{g,q}^k\right] \tag{14}$$

where $\mathbf{Z}$ is the breakpoint sensitivity matrix. The matrix $\mathbf{Z}$ is composed by submatrix blocks of 3×3 dimensions, as the three-phase system is considered. The block $\mathbf{Z}_g$ is formed by the adding the series impedances of the distribution lines linking the substation and the DG at bus g. In such case, the impedance matrix of the DG ($\mathbf{Z}_{DG}$) is considered. Otherwise, the submatrix $\mathbf{Z}_q$ is created by adding the impedances of the lines linking the buses q and q'. Finally, $\mathbf{Z}_{gq}$ is composed by the addition of the common lines of submatix $\mathbf{Z}_g$ and $\mathbf{Z}_q$.

Also, in Eq. (13), $\mathbf{E}_g^k$ is the internal voltage for dispersed generators based in synchronous machine or in electronically interfaced unit. This voltage represents the internal state of the generator due to operational condition at the common point with the distribution system. Hence, for the k-th iteration of the algorithm, the Eq. (15) is used to calculate $\mathbf{E}_g^k$, where $\mathbf{J}_g^k$ is the three-phase currents vector of the DG connected at bus g, and $\mathbf{V}_{ng}^k$ is the voltage difference at the grounded impedance of the generator.

$$\left[\mathbf{E}_g^k\right] = \left[\mathbf{V}_g^k\right] + [\mathbf{Z}_{GD}]\left[\mathbf{J}_g^k\right] + \left[\mathbf{V}_{ng}^k\right] \tag{15}$$

In addition, in Eq. (13), $\mathbf{E}_g$ is a reference vector of the internal voltage of the generator. This vector of three-phase balanced voltage represents the necessary internal condition to match the scheduled criteria for the generator. The Eqs. (16) and (17) are used to calculate the vector $\mathbf{E}_g$, where $\mathbf{V}_g^1$ is a positive-sequence component of vector $\mathbf{V}_g^k$. $Pesp_g$ and Q_g^k are the active and reactive power scheduled for generator connected at bus g of the distribution system, respectively.

$$\mathbf{E}_g = \begin{bmatrix} 1 & 1 & 1 \\ 1 & a^2 & a \\ 1 & a & a^2 \end{bmatrix} \begin{bmatrix} 0 \\ E_g^1 \\ 0 \end{bmatrix} \tag{16}$$

where:

$$E_g^1 = V_g^1 + X_1\left(\frac{P\mathrm{esp}_g + jQ_g^k}{V_g^1}\right) \tag{17}$$

The reactive power at Eq. (17) must be adjusted at each iteration when the operation mode of the DG is set to a PV bus. In this case, the reactive power is controlled to guarantee a specified voltage, $\mathbf{V}esp_g$. Hence, the Eq. (18), proposed in (Shirmohammadi et al. 1988), is used to calculate the increasing vector of the reactive power for each generator with voltage control, $\Delta\mathbf{Q}_g$. In this equation, the matrix $\mathbf{X}$ is the sensitivity matrix with the positive-sequence reactances of the submatrix $\mathbf{Z}_g$ (see Eq. (13)). However, the internal reactances of the DG are not included in the creation of the matrix $\mathbf{X}$.

$$[\mathbf{X}]\left[\Delta\mathbf{Q}_g\right] = \left[\mathbf{V}_g^1 - \mathbf{V}\mathrm{esp}_g\right] \tag{18}$$

Once the Eq. (18) is solved, the new value for the reactive power injected for each generator with voltage control is calculated with the Eq. (19).

$$Q_g^k = Q_g^{k-1} + \Delta Q_g \tag{19}$$

Furthermore, Eqs. (20) and (21) bind the internal voltage and the reactive power of the DG connected at bus g, respectively. These limits aim to find a feasible solution for the operation of the generator. The first one limits the exciting current in the field winding. The second one looks for a limited current flowing for the armature of the machine.

$$E_g^{\min} \leq E_g^1 \leq E_g^{\max} \tag{20}$$

$$Q_g^{\min} \leq Q_g \leq Q_g^{\max} \tag{21}$$

When the reactive power matches one of its operational limits, the control mode for the generator turns into a PQ bus. The same idea applies when the internal voltage reaches either the lowest or highest values. In turn, the limits for the internal voltage can be estimated in terms of the setting parameters of the generator. To attempt this, the Eq. (17) can also be applied. In such case, we set $Pesp_g = P_g^{max}$ and $Q_g = Q_g^{max}$ to calculate E_g^{max}. Meanwhile, $Pesp_g = P_g^{min}$ and $Q_{GD} = Q_{GD}^{min}$ is settled to estimate E_g^{min}. Summarizing, Fig. 5 sketches a flowchart for the deterministic algorithm of load flow implemented in this paper.

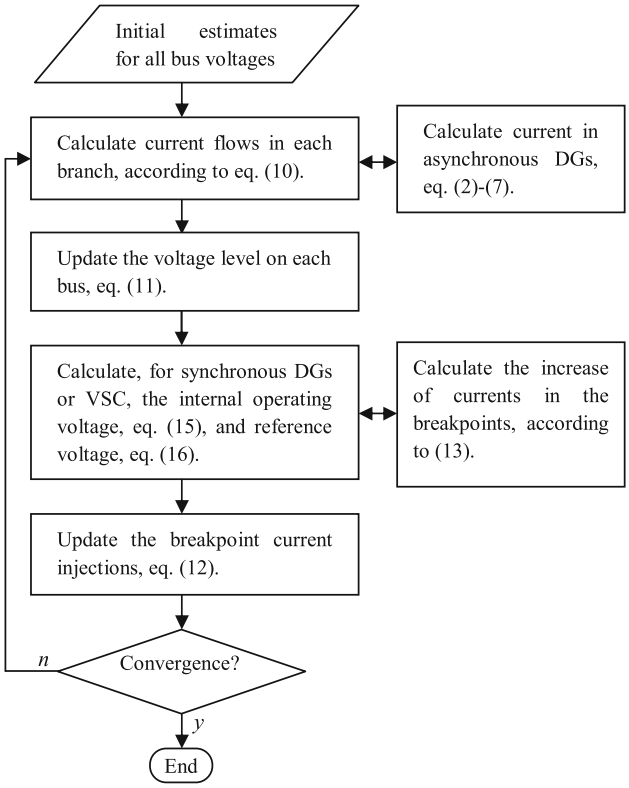

Fig. 5 Load-flow algorithm

4 Short-Circuit Algorithm

The implemented algorithm for short-circuit calculation was initially proposed in (Zhang et al. 1995). This algorithm is based in the compensation theory described in Sect. 3. However, in this paper, some modifications aim to improve the algorithm and enhance its capability.

The intensity of the short-circuit current in any distribution system depends of many factors. One of them is the ground impedance, i.e., the impedance between the conductor element and the earth surface. In this paper, the algorithm proposed in (Zhang et al. 1995) is used for short-circuit purposes. However, this algorithm does not consider ground impedance. This assumption produces higher intensity values of the short-circuit currents. Hence, it is very unlikely the generation of short-circuit currents with precision enough to estimate the correct tripping of protective devices.

As the compensation theory is implemented to calculate the short-circuit currents, the sensitivity matrix presented in Eq. (13) can be used again. However, in this case, the closed path created between the point fault and the substation must be added. So, the enhanced matrix system in Eq. (22) is used to calculate the increasing currents in all the breakpoints, i.e., DGs, circuit loops, and short-circuit faults.

$$\begin{bmatrix} \mathbf{Z}_g & \mathbf{Z}_{gq} & \mathbf{Z}_{gf} \\ \mathbf{Z}_{gq} & \mathbf{Z}_q & \mathbf{Z}_{qf} \\ \mathbf{Z}_{gf} & \mathbf{Z}_{qf} & \mathbf{Z}_f \end{bmatrix} \begin{bmatrix} \Delta\mathbf{J}_g^k \\ \Delta\mathbf{J}_q^k \\ \Delta\mathbf{J}_f^k \end{bmatrix} = \begin{bmatrix} \mathbf{E}_g^k - \mathbf{E}_g \\ \mathbf{V}_{q'^k} - \mathbf{V}_q^k \\ \Delta\mathbf{V}_{f^k} \end{bmatrix} \tag{22}$$

The new submatrixes in the enhanced sensitivity matrix are constructed with the same philosophy as described below in Sect. 3.3. The submatrix $\mathbf{Z}_f$ is the summation of the impedances of the lines linking the substation with the fault point. The equivalent impedance of the transmission system and the substation can be taken into account inside the submatrix $\mathbf{Z}_f$. Furthermore, the block $\mathbf{Z}_{gf}$ is the sum of the series impedance of the lines used in creating both matrixes $\mathbf{Z}_g$ and $\mathbf{Z}_f$. The same idea is implemented for block $\mathbf{Z}_{qf}$, but analyzing the matrixes $\mathbf{Z}_q$ and $\mathbf{Z}_f$.

In order to include the fault impedance into the formulation, we first show the example sketched in Fig. 6. In such figure, a three-phase short-circuit is assumed at bus f of the distribution system. Since the fault is drained through the impedance Z_n, a voltage difference V_n is created, and the current J_n flows through the fault impedance.

Hence, the matrix system (23) describes the equivalent impedance of Thévenin at the fault point f. The first matrix is the sum of all the lines linking the substation and the bus f. Meanwhile, the second matrix incorporates the effect of the fault impedance.

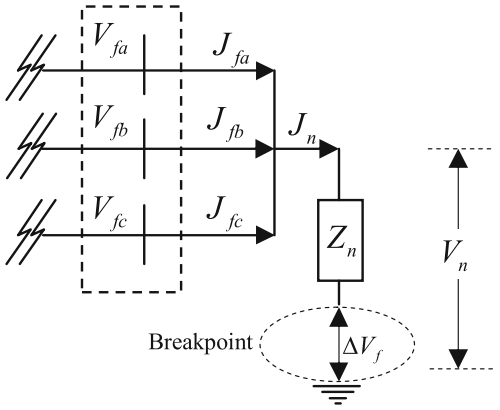

Fig. 6 Short-circuit breakpoint

$$\mathbf{Z}_f = \begin{bmatrix} Z_{aa} & Z_{ab} & Z_{ac} \\ Z_{ba} & Z_{bb} & Z_{bc} \\ Z_{ca} & Z_{cb} & Z_{cc} \end{bmatrix} + \begin{bmatrix} Z_n & Z_n & Z_n \\ Z_n & Z_n & Z_n \\ Z_n & Z_n & Z_n \end{bmatrix} \tag{23}$$

To obtain the mismatch of the three-phase voltage at the fault point $\Delta\mathbf{V}_{f^k}$, the Eq. (24) is applied at each iteration of the algorithm.

$$\Delta\mathbf{V}_{f^k} = \begin{bmatrix} V_{fa}^k - Z_n \cdot \left(J_{fa^k} + J_{fb^k} + J_{fc^k}\right) \\ V_{fb}^k - Z_n \cdot \left(J_{fa^k} + J_{fb^k} + J_{fc^k}\right) \\ V_{fc}^k - Z_n \cdot \left(J_{fa^k} + J_{fb^k} + J_{fc^k}\right) \end{bmatrix} \tag{24}$$

In addition, the implemented algorithm is modified to consider the impact on the short-circuit current from asynchronous generator units. From a general point of view, in a transitory state, one fault creates a low voltage profile in a whole distribution system, and such condition reduces the magnetizing current of asynchronous machines. Hence, asynchronous generators can be disregarded in transitory studies of short-circuit. A similar idea can be applied at DGs with electronically-interfaced units, in which the controls lead to a fast disconnection of the unit a few cycles before the fault incidence (Boutsika and Papathanassiou 2008). However, in subtransitory state, the remanent magnetization in the core has a significant contribution in the short-circuit intensity. For this reason, in this paper, the asynchronous generators are treated as synchronous machines when subtransitory studies are made. To attempt this, we set $X_2 = X_0 = 0$ and $X_1'' = X_s + X_r$ (Anderson 1998) and the modeling of Sect. 2.1 is applied, instead of the application of the model described in Sect. 2.2.

In the calculation of the mismatch vector of three-phase voltage, the internal voltage of generators is settled as a constant parameter. Therefore, $\mathbf{E}_g$ depends on the state operation in which the fault is presented. Thus, Eq. (25) is used for subtransitory studies, and Eq. (26) is employed for transitory studies (Anderson 1998). It is observed that in both cases the internal tension is a function of the level voltage

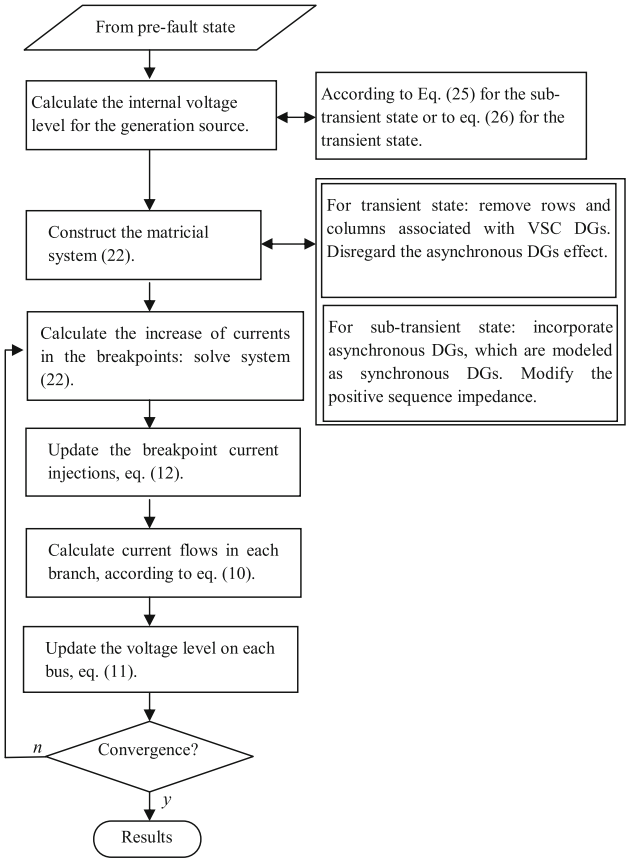

Fig. 7 Flowchart for short-circuit algorithm

at terminals of the generator ($\mathbf{V}_g$), and the current flowing through the armature windings ($\mathbf{J}_g$) during the pre-fault condition.

$$\left[\mathbf{E}_g''\right] = \left[\mathbf{V}_g\right] + \left[\mathbf{Z}_{GD}''\right]\left[\mathbf{J}_g\right] \tag{25}$$

$$\left[\mathbf{E}_g'\right] = \left[\mathbf{V}_g\right] + \left[\mathbf{Z}_{GD}'\right]\left[\mathbf{J}_g\right] \tag{26}$$

The matrix $\mathbf{Z}_{GD}''$ and $\mathbf{Z}_{GD}'$ are both calculated through Eq. (1). However, the reactance of the positive-sequence sets a value in accordance with the time in which the short-circuit is calculated. Hence, in a subtransitory study, X_1 is set to X''^1, i.e., the subtransitory direct-axis reactance of the generator. Meanwhile, in a transitory study, X_1 is set to a transitory direct-axis reactance X'^1. Obviously, the above criteria also must be considered into the $\mathbf{Z}_g$, from Eq. (22), in order to keep coherence.

Summarizing, in Fig. 7 the flowchart of the implemented algorithm for short-circuit analyses is depicted. It must be noted that once Eq. (22) is solved, the algorithm performs one iteration of the radial power flow to determine the distribution of the current flows.

5 Point Estimate Method

In this paper, the probabilistic analysis is based on a particular case of the Point Estimate Method, which is known as Three-Point Estimate Method (Hong 1998). This method will lead with uncertain parameters involved in the calculation of power load flow and short-circuit currents. The Three-Point Estimate Method (TPEM) was selected instead of the traditional Monte Carlo Method (MCM) proposed in (Rubinstein 1981), since the TPEM has a low computational effort and a similar convergence when compared with the MCM.

The TPEM performs an estimated behavior of a set of uncertain output parameters **W**. This behavior is related to the interaction of a set of entries **X** into a plant described by the transfer function $h(\mathbf{X})$, where at least n parameters into the set **X** have uncertain behavior.

To attempt the estimated behavior of **W**, the algorithm concentrates the probabilistic information in only three points by each random variable, which are denoted by x_{ki} with $i = 1, 2, 3$ and $k = 1, 2, ..., n$. Each concentration x_{ki} is placed to a distance ξ_{ki} from the mean value μ_k, which in turn depends on the first four statistical moments of the self variable, i.e., the mean value μ_k, the standard deviation (SD) σ_k, the asymmetry coefficient λ_{k3}, and the kurtosis coefficient λ_{k4}. Hence, the Eq. (27) is used to determine the concentration value,

$$x_{ki} = \mu_k + \xi_{ki} \cdot \sigma_k \tag{27}$$

where ξ_{ki} is calculated with the Eq. (28) when $i = 1, 2$:

$$\xi_{ki} = \frac{\lambda_{k3}}{2} + (-1)^{3-i} \sqrt{\frac{\lambda_{k4}}{2} - 3\left(\frac{\lambda_{k3}}{2}\right)^2} \tag{28}$$

and the Eq. (29) is used when i = 3.

$$\xi_{k3} = 0 \tag{29}$$

The Eq. (29) sets all the variables in the mean value. Thus, the algorithm needs to determine only $2n$ deterministic scenarios by each random variable, plus an additional scenario in which all variables are set in the mean value. As the number of scenarios to be calculated is significantly reduced if compared to the traditional MCM, the algorithm leads to a low computational requirement and fast response capability.

When all scenarios are evaluated, the algorithm uses Eq. (30) to determine the mean value of the output variables.

$$E(\mathbf{W}) = \sum_{k=1}^{n} \sum_{i=1}^{3} p_{ki} \cdot h\left(\mu_1, \mu_2, \ldots, x_{ki}, \ldots, \mu_n\right) \tag{30}$$

where p_{ki} is the probability value of the k-th concentration, which is calculated by Eq. (31) when i = 1,2, or by Eq. (32) when i = 3.

$$p_{ki} = \frac{(-1)^{3-i}}{\xi_{ki} \cdot (\xi_{k1} - \xi_{k2})} \tag{31}$$

$$p_{ki} = \frac{1}{n} - \frac{1}{\lambda_{k4} - \lambda_{k3}^2} \tag{32}$$

And the SD for each output variable is calculated by Eq. (33).

$$\sigma_{\mathbf{W}} = \sqrt{\sum_{k=1}^{n} \sum_{i=1}^{3} p_{ki} \cdot h\left(\mu_1, \mu_2, \ldots, x_{ki}, \ldots, \mu_n\right) - E^2(\mathbf{W})} \tag{33}$$

The algorithm implemented in this paper for probabilistic analysis is enabled to deal with independent random variables. If the variables into the set **X** exhibit some correlation, a transformation must be applied. For example, in (Morales et al. 2010) one eigenvalues-based transformation is described, which creates an equivalent system of independent random variables from a set of correlated variables.

Summarizing, a flowchart of the probabilistic algorithm for load flow calculation and short-circuit analysis is proposed in this paper is shown in Fig. 8.

6 Results

The PA was implemented in a personal computer Dell with Intel Core i7. All the routines were developed in Delphi 7. Two test systems with different complexity are used to show the advantage of the PA.

6.1 Deterministic Algorithms

In order to show the advantage of the PA, the deterministic algorithms described in this paper were tested in a simple 11 bus test system shown in Fig. 9. The voltage level of the system is set to 4.16 kV, as the system distribution lines are represented by the impedance matrix described in the Table 1.

The asymmetric fashion showed by the impedance matrix enables the uses of sequence components and the implementation of the software Neplan (NEPLAN 2012). The load demand of the test system is described in the Table 2, where a Y-grounded connection and a constant power modeling are assumed for all loads.

DGs are usually connected to the grid through Y-grounded/Delta transformers to isolate zero-sequence currents. Hence, an interfaced-transformer synchronous generator is connected to the grid in bus 10 of the distribution system.

In Fig. 10 the voltage profile in buses of the distribution system is shown. The results obtained through implementing the PA are compared with values obtained in a Neplan simulation. Furthermore, two different generator modeling

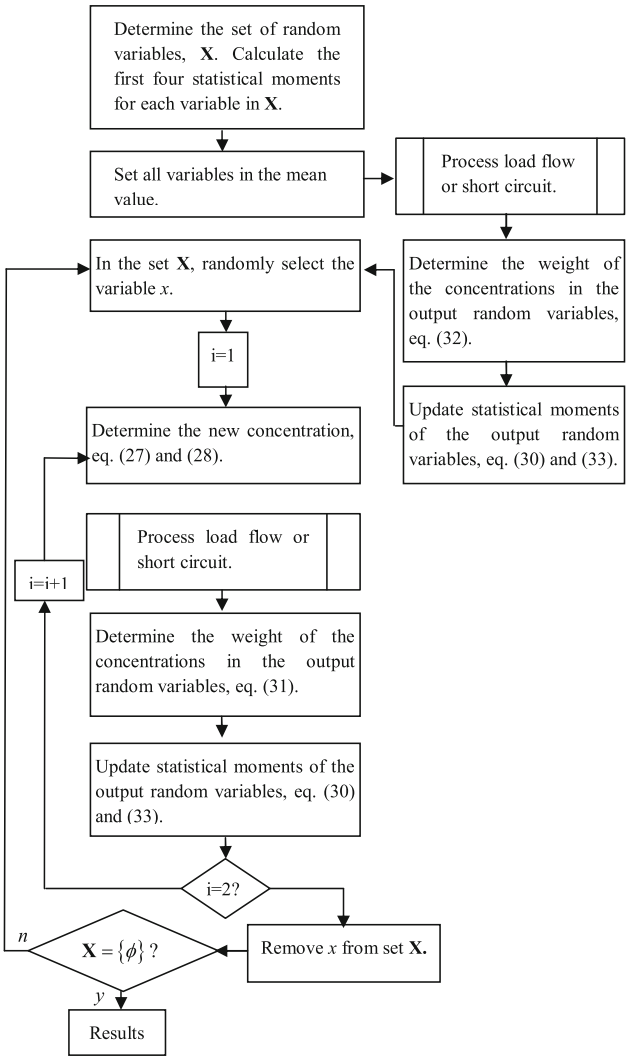

Fig. 8 Flowchart of the PA for probabilistic analysis

Table 1 Impedance matrix of distribution line (ohm/km)

	A	B	c
a	0.3465 + j1.0179	0.1560 + j0.4236	0.1560 + j0.4236
b	0.1560 + j0.4236	0.3465 + j1.0179	0.1560 + j0.4236
c	0.1560 + j0.4236	0.1560 + j0.4236	0.3465 + j1.0179

are implemented into the PA. The first one is the proposed modeling (PM) described in Sect. 2 of this paper. The second one is the negative power load (Pneg) modeling traditionally described in academic papers.

In Fig. 10 it is noted that the relative error of the results obtained with Pneg modeling is around 3.41 % if compared with Neplan results. Instead, the relative error was around 0.12 % when PM is used.

The Fig. 11 shows the results for the current flow at terminals of the DG. It is easy to observe that Pneg modeling

Table 2 Load demand (kVA)

Bus	Phase A	Phase B	Phace C
2	8.5 + j5.0	33.0 + j19.0	58.5 + j34.0
3		170.0 + j125.0	
4	160.0 + j110.0	120.0 + j90.0	120.0 + j90.0
5		230.0 + j132.0	
6	393.5 + j225.0	418.0 + j239.0	443.5 + j254.0
7			170.0 + j151.0
9			170.0 − j20.0
10	485.0 − j10.0	68.0 − j140.0	290.0 + j12.0
11	128.0 + j86.0		

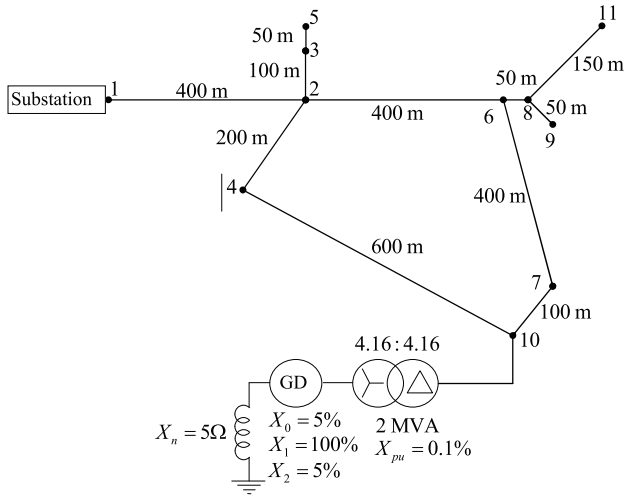

Fig. 9 Eleven bus test system

creates a balanced condition in the magnitude of the currents. This situation could lead to mask overload conditions in both distribution lines and generator windings.

Furthermore, Fig. 12 is employed to show the three-phase voltage profile when an asynchronous generator is connected to the grid through a Y-grounded/Delta transformer. In this case, the upper value of the relative error was 0.17 % when compared with results obtained with Neplan. It must be remarked that *Pneg* modeling does not have an implicit methodology to determine the reactive power consumed by asynchronous generators. In such case, the reactive power is calculated on the basis of the load power factor at nominal settings. For this reasons, it is not possible to consider a direct comparison between the *PM* and the *Pneg* modeling.

Finally, Table 3 shows the results for short-circuit currents at bus 9 of the distribution system. In this analysis, it is assumed different fault impedance values and the impact on the short-circuit current is calculated. For each case, the pre-fault condition described in Fig. 9 is assumed. The sub-transitory direct-axis impedance for generator is $X''^{1} = 0.20$

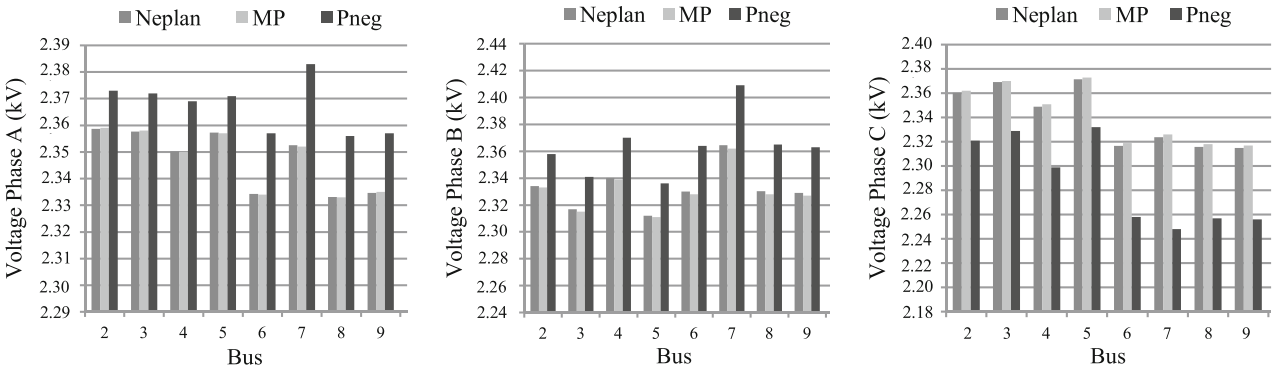

Fig. 10 Voltage profile comparison as a function of the DG model

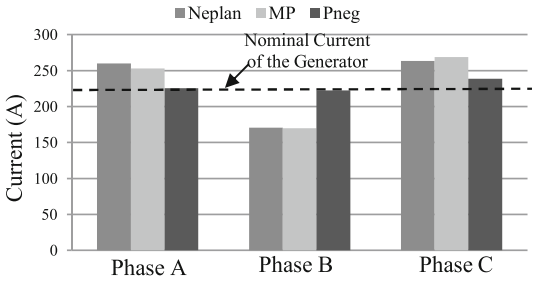

Fig. 11 Three-phase generator current as a function of the generator modeling

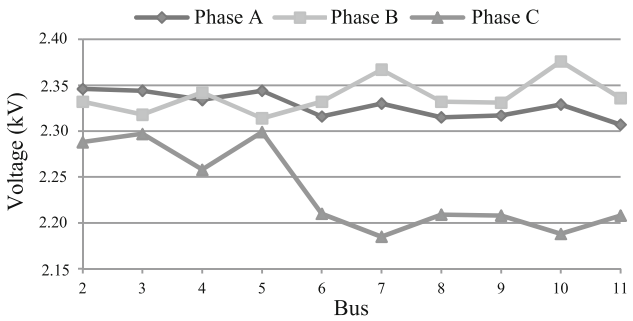

Fig. 12 Three-phase voltage profile at terminals of the asynchronous generator

pu. From the results showed in Table 3 it is easy to note a high impact on the short-circuit current as the fault impedance decreases. In addition, at each scenario the PM shows a similar value when compared with to those obtained by the software Neplan. The upper value of the relative error was 5.7 %.

The addition of the fault impedance in the PA could be crucial for calculating the short-circuit current in distribution system, since the real behavior of the currents can be estimated with major accuracy. This issue is reasonably important in protective device coordination studies that require the determination of current values with enough precision to estimate the tripping of protective devices.

Table 3 Short-circuit current (A) for a single-phase fault at phase A of the bus 9 of the distribution system

Fault impedance (Ω)	Neplan	MP
0	3,484	3,522
10	226	239
20	115	121
30	77	81
40	58	61

6.2 Probabilistic Load Flow

The modified IEEE 123 bus test system was used to verify the efficiency of probabilistic methodology proposed in this paper. The system has a higher complexity than the 11 bus test system used in Sect. 6.1, because the system has a greater number of buses, an untransposed three-phase feeders, and single-phase laterals. For this reason, the analysis in sequence components is inadequate since the coupling between sequence circuits are generated at the transforming process.

The substation operates at 4.16 kV and the database for both load demand and distribution lines is available in (Kersting 1991). Figure 13 shows the topology of the distribution system. The voltage regulators and transformers initially installed in the distribution system were not considered. In this paper, these devices were replaced by closed switches to visualize what the impact of DGs on distribution system is. The state of both the control and protective devices described in (Kersting 1991) is assumed. Initially, no DG is connected to the grid, but in addition to the condition laid out in the database, a load demand with uncertain behavior is considered. This behavior will be described by a normal distribution with mean value equal to the database and SD of 10 %.

From the point of view of the TPEM implementation, the set **X** of uncertain parameters entering to the load-flow algorithm is composed by both the active and reactive power

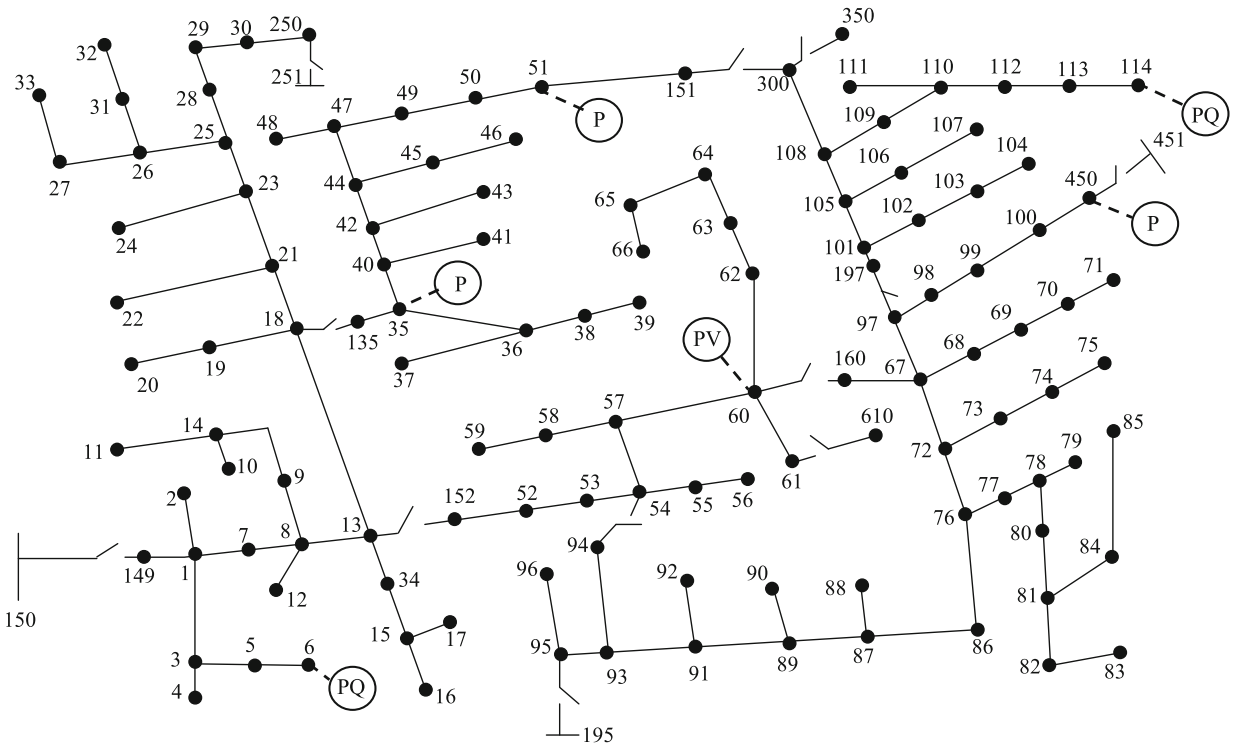

Fig. 13 Modified IEEE 123 bus test system

delivered and consumed by DGs and load demand, respectively. Meanwhile, the set **W** of output variables is related to the magnitude of the three-phase voltage at each bus of the distribution system. Hence, the transfer function h(**X**) is related to the deterministic load-flow calculation described in this paper. To validate the results obtained by the PA, the Monte Carlo Simulation Method (MCM) was implemented as well, in which 10,000 iterations were assumed as convergence criteria. Furthermore, results from a MCM simulation were set as a benchmark solution.

Results of the output variables were significantly similar when both the PA and the MCM were applied. The upper value of the relative error in the mean value of the voltage level, considering all distribution buses, was 0.00136 %. In addition, the upper value in the SD was around of 4.06 %. However, the PA converged 20 times faster than MCM. For this reason, the PA could be considered more efficient and with the same accuracy as the MCM. Figure 14 shows the mean value of the voltage magnitude at all buses of the distribution system. These results were obtained through the algorithm proposed in this paper.

The proposed methodology can be extended to consider the impact of renewable sources. To demonstrate this advantage, six DGs were connected to the modified IEEE 123 bus test system, as shown in Table 4. The first type of DG consists of synchronous generator with both voltage and active power controller. The second type consists of an asynchro-

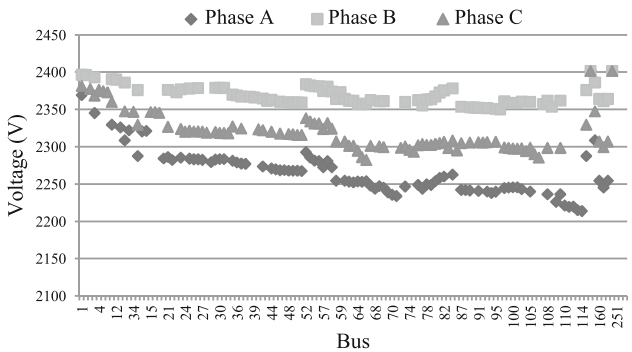

Fig. 14 Voltage profile with no DGs connected

nous generator-based wind source with active power control, as described in Sect. 2. Finally, the third type of generator is an electronically interfaced photovoltaic source with unity power factor controller. The first and the second types of generators are three-phase source. Conversely, the third type of generator is a single-phase source. All DGs operate at 4.16 kV, and their parameters are referenced to the nominal setting of the generator.

The active power delivered by wind generators depend on the wind speed at the location of the facility. At real conditions, the wind speed exhibits an uncertain behavior that must be considered in the PA. In academic literature, the wind speed is modeled as a probabilistic variable defined by

Table 4 DGs connected to the system

Type	Bus	Control	P_{nom} [kW]	Q_{nom} [kVa]	Parameters [pu]
1	60	PV	1,200	500	$X_0 = 0.05j$ $X_1 = 1.10j$ $X_2 = 0.12j$
2	51 35 450	P	1,200	−300	$R_s = R_r = 0.05$ $X_s = X_r = 0.16j$ $X_m = 13j$
3	6 114	PQ	30	0	$X_1 = 0.1j$

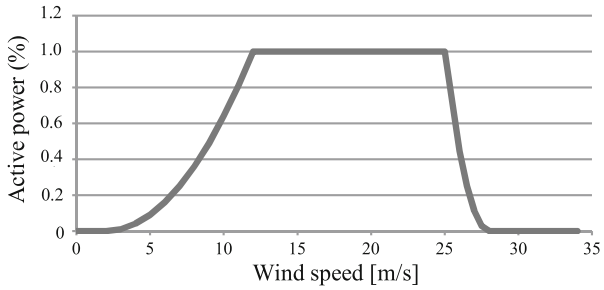

Fig. 15 Active power function (pu) for wind generators

a Weibull Distribution Function. Hence, it is considered that the shape factor of such function has a value of 2, as the scale factor is set at 10. The active power control of wind generators, as a function of the wind speed, is generally represented as shown Fig. 15. Meanwhile, the reactive power at the same source depends on the circuit parameters and the voltage at terminals of the generator, such as described in Sect. 2.2 of the present paper.

As assumed in wind generation, it is considered that the active power delivered by photovoltaic sources can be modeled as a weibull distribution function with shape factor equal to 2, and scale factor equal to 15. This modeling attempts to simulate the variation of the incident luminosity at the photovoltaic cells.

The Fig. 16 shows the mean value of the voltage magnitude at all buses of the distribution system when DG connection is considered. These results were obtained with the PA implementation. At this scenario, the upper mismatch with results obtained with MCM reaches a value equal to 0.032 %. Meanwhile, the SD had a mean mismatch around of 3.582 %. The time covered in processing the proposed probabilistic power flow was 50 times lower than the time consumed with MCM.

Figure 16 points out the three-phase voltage magnitude at the location of the controlled-voltage DG. It is possible to verify that DG can control the voltage magnitude at its terminals even with fluctuations in the other sources. At this scenario, the positive- sequence voltage had a magnitude around 99.93 % of the scheduled voltage.

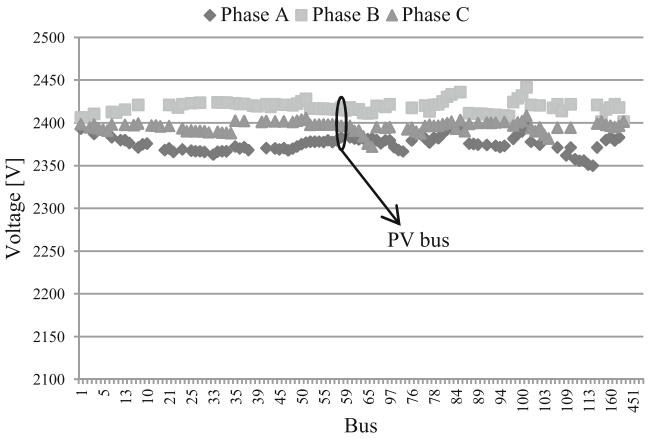

Fig. 16 Voltage profile considering DG connected to the grid

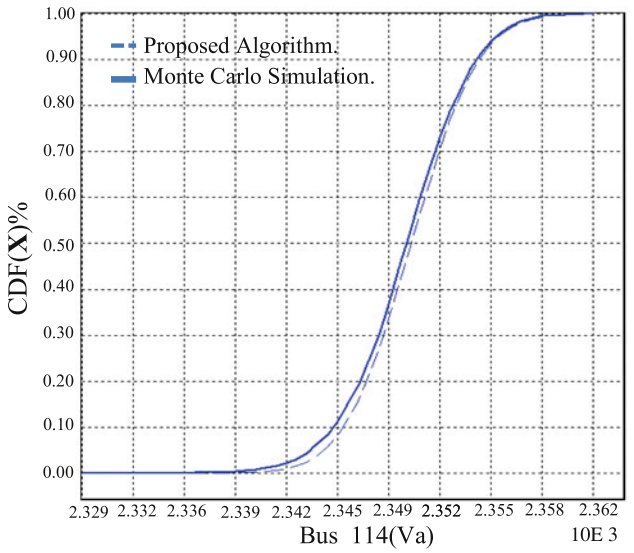

Fig. 17 CDF of the voltage magnitude at phase A of the bus 114

Results obtained with the PA show that voltage magnitude at all buses of the distribution system has a low probability to reach a voltage lower than 2.281 kV (95 % of the desired voltage). So, the viability of adequate control of voltage magnitude is proved. This fact can be verified in Fig. 17, where a Cumulative Distribution Function (CDF) for voltage magnitude at phase A of bus 114 is depicted (At the analyzed scenario, the phase A of the bus 114 had the lowest voltage magnitude). In this figure, the solid line is related to the behavior calculated with the MCM, while the dashed line represents results of the PA.

6.3 Probabilistic Short-Circuit

Actually, there are many factors involved in the short-circuit calculation, such the operation point of both load demand and

generators, the topology of the distribution system, the fault location, and, mainly, the fault impedance. This last parameter, in turn, depends on multiple variables with uncertain behavior, such as the temperature of the environment surrounding the conductors, the moisture and the physical composition of the ground, and others (IEEE Std 551-2006 2006). Consequently, the fault impedance must be modeled as a random variable with a defined probability distribution function, which can be estimated regarding the conditions around the fault location. In accordance with the above statement, the PDF could be a consequence of probabilistic studies of database with the short-circuit currents which affected the distribution system in the past.

Hence, the PA was tested through a simulation of a single-phase fault at phase A of the bus 114 of the modified IEEE 123 bus test system. The fault impedance was considered as a resistance with random value. Consequently, the value of this new uncertain parameter was based in a Weibull PDF with shape factor equal to 2.5, and a scale factor equal to 40. At the presented scenario, the impact on the current sensed by a protective device placed at the branch linking the buses 108 and 109 was analyzed.

In addition to the fault impedance, the set **X** of probabilistic parameters is formed by the active and reactive power consumed by the load demand, as well as the active and reactive power delivered by DGs connected to the grid. Conversely, the set **W** of output variables is composed only by short-circuit current at the branch linking the buses 108 and 109. Finally, the transfer function h(**X**) is based on the deterministic short-circuit algorithm described in Fig. 5.

The implemented methodology found that the short-circuit current has a mean value equal to 126.5 A, while the SD was estimated in ±45.4 A. Such values, when compared with values obtained with MCM, had a relative error equal to 4.1 and 23.7 %, respectively. To evidence this behavior more clearly, Fig. 18 shows a CDF of the output variable. In this figure, results from both implemented methodologies, PA and MCM, are presented.

In Fig. 18, when a single-phase fault happens at bus 114, the highest value in the short-circuit current that could be experimented by the protective device is 1,100 A. However, this magnitude has a low probability to happen and it is related to solid- impedance fault. This fact is crucial for sizing of interrupting capacity of the protective device.

In addition, there is a 50 % probability that current flowing over the protective device, during the fault condition, would be lower than the mean value calculated. To accomplish a better calibration of the protective device, it is necessary to consider values lower than 126 A. However, the current triggering the protective device must be sufficiently higher than the steady state current (which is estimated in 65 A, according with the implementation of the deterministic power described in the Fig. 5).

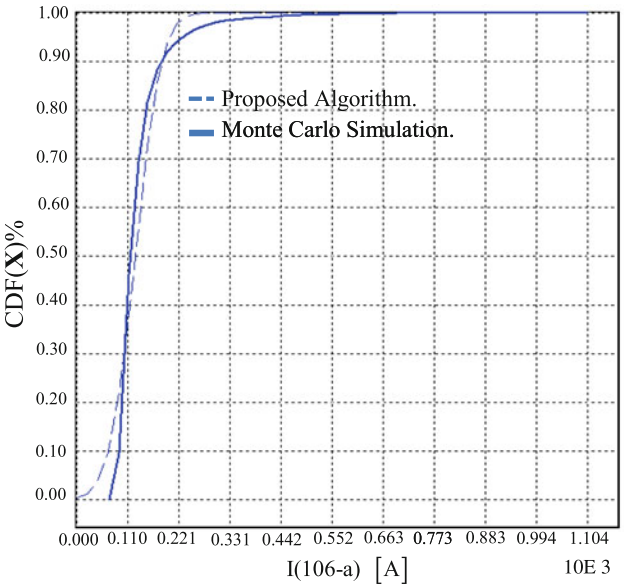

Fig. 18 CDF for the short-circuit current at phase A of the bus 114

Table 5 Computational effort for scenario (seconds)

Scenario	MPP	Monte Carlo
Load flow without DG	0.437	9.776
Load flow with DG	0.545	28.41
Short-circuit analyzes with DG	0.847	36.332

Thus, the PA gives additional information to decide the adequate setting of the protective device, and the planning engineer could be more confident around the proper coordination and selectivity of the protection project.

6.4 Computational Effort

As mentioned before, the implemented methodology has great advantage when compared with traditional approach. To visualize this advantage, the computational time needed at each simulation is exposed in Table 5.

7 Conclusion

The impact on the load-flow results with different DG modeling was studied. From the models considered, we believe that the proposed modeling could reflect more precisely the real behavior of DG connected to grid, as the internal parameters of the generator are regarded. However, the efficiency of the algorithm is not affected.

A probabilistic algorithm for load-flow calculation and short-circuit analysis is proposed. The algorithm proved to be efficient when applied in weakly meshed distribution sys-

tems. The time required for one probabilistic analysis can be reduced at least 50 times lower than the time consumed by traditional methodologies, such as Monte Carlo Simulation. Despite this reduction, the quality of the results was not affected significantly.

The test systems were focused in uncertain variables in load demand and generation. However, for the sake of generality, the methodology can be expanded to consider uncertainty in other kind of parameters.

The proposed methodology can analyzes different kind of scenarios in an efficient and accurate way. Thus, the PA can aggregate information to generate a clear understanding about the operation of DGs connected to the grid and support decisions in planning distribution systems.

The implementation of both a three-phase load flow and an adequate DG modeling enable a better estimation of the impacts on the distribution system when DGs are the connected to the grid. In the modeling of DGs, it is important to consider the technology and control of the generator.

The high efficiency of the proposed methodology facilitates the implementation in planning studies of distribution system with DG connected, where several scenarios must be analyzed to determine the optimal operation of the grid. When probabilistic information is considered, the algorithm can estimate the probability that some event might happen. Although the PA can estimate with precision the first three statistical moments, there can be an implicit error when estimating values different from the mean value. This issue is due to the fact that PA cannot identify the appropriate probability distribution function of the output variables. However, despite the assumption of a normal distribution, the implicit error is so miniscule that it could be disregarded in distribution planning studies. A possible implementation of the PA may be used to minimize the risk of getting voltage values outside the acceptable range, for any bus in the distribution system. On the other hand, in order to reduce the error induced by the normal distribution approximation, a methodology based on the third statistical moment could be formulated to evaluate asymmetric distributions.

Acknowledgments The authors thank the support granted by FAPESP (Proc. 2009/00296-1 and Proc. 2009/53841-7), and by (Proc. 302272/2009-7).

References

Abdel-Akher, M., Mohamed, K., & Abdul, R. A. H. (2005). Improved three-phase power flow methods using sequence components. *IEEE Transactions on Power Systems*, *20*(3), 1389–1396.

Anderson, P. M. (1998). *Analysis of faulted power systems*., IEEE Press Power Systems Engineering Series London: Wiley.

Balaguer, I. J., Shuitao, Q. L., Suppatti, U., & Peng, F. (2011). Control for grid-connected and intentional islanding operations of distributed power generation. *IEEE Transactions on Industrial Electronics*, *58*(1), 147–157.

Baran, M., & Staton, E. (1997). Distribution transformer models for branch current based feeder analysis. *IEEE Transactions on Power Systems*, *12*(2), 698–703.

Bordalo, U. A., Rodrigues, A. B., & Da Silva, M. G. (2006). A new methodology for probabilistic short-circuit evaluation with applications in power quality analysis. *IEEE Transactions on Power Systems*, *21*(2), 474–479.

Boutsika, T., & Papathanassiou, S. (2008). Short circuit calculations in networks with distributed generation. *Electric Power Systems Research*, *78*(7), 1181–1191.

Brahma, S. M., & Adly, A. G. (2004). Development of adaptive protection scheme for distribution systems with high penetration of distributed generation. *IEEE Transactions on Power Delivery*, *19*(1), 56–63.

Chen, B. K., Chen, M.-S., Shoults, R., & Liang, C. C. (1990). Hybrid three phase load flow. *IEE proceedings*, *137*(3), 177–185.

Cheng, C. S., & Shirmohammadi, D. (1995). A three-phase power flow method for real-time distribution system analysis. *IEEE Transactions on Power Systems*, *10*(2), 671–679.

Chun-Lien, S. (2005). Probabilistic load-flow computation using poit estimate method. *IEEE Transactions on Power Systems*, *22*(4), 1843–1851.

Chun-Lien, S. (2010). Stochastic evaluation of voltages in distribution networks with distributed generation using detailed distribution operation models. *IEEE Transactions on Power Systems*, *25*(2), 786–795.

Gallego, L. A., Granada, E. M., & Padilha-Feltrin, A. (2012). Fluxo de potência trifásico probabilístico para redes de distribuição usando o método de estimação por pontos. *Sba Controle & Automação*, *3*(2), 179–189.

Granada, E. M., Rider, M. J., & Mantovani, J. (2010). Mathematical decomposition technique applied to the probabilistic power flow problem. Transmission and Distribution Conference and Exposition pp. 139–146.

Hong, H. P. (1998). An efficient point estimated method for probabilistic analysis. *Reliability Engineering and System Safety, Barking*, *59*(3), 261–267.

IEEE Std 551–2006. (2006). Recommended practice for calculating short-circuit currents in industrial and commercial power systems. Retrieved Jul 2011 from http://ieeexplore.ieee.org/servlet/opac?punumber=4015544.

Kersting, W. H. (1991). Radial distribution test feeders. *IEEE Transactions on Power Systems*, *6*(3), 975–985.

Kosterev, D. (1997). Modeling synchronous voltage source converters in transmission system planning studies. *IEEE Transactions on Power Delivery*, *12*(2), 947–952.

Morales, J., Baringo, L., Conejo, A., & Mínguez, R. (2010). Probabilistic power flow with correlated wind sources. *IET Generation, Transmission and Distribution*, *4*(10), 641–651.

NEPLAN. (2012). Power systems analysis and engineering. Retrieved May 2012 from http://www.neplan.ch.

Pepermans, G., Driesen, J., Haeseldonnckx, D., Belmans, R., & D'haeseleer, W. (2001). Distributed generation: definition, benefits and issues. *Electric Power System Research*, *57*(3), 195–204.

Rubinstein, R. Y. (1981). *Simulation and the Monte Carlo Method*. London: Wiley.

Shirmohammadi, D., Hong, H., Semlyen, A., & Luo, G. X. (1988). A compensation-based power flow method for weakly distribution and transmission networks. *IEEE Transactions on Power Systems*, *3*(2), 753–762.

Tinney, W. F. (1972). Compensation methods for networks solutions by triangular factorization. *IEEE Transactions on Power Apparatus and Systems, PAS*, *91*(1), 123–127.

Zakaria Kamh, M., & Iravani, R. (2010). Unbalanced model and power-flow analysis of microgrid and active distribution systems. *IEEE Transactions on Power Delivery*, *25*(4), 2851–2858.

Zhang, X., Soudi, F., Shirmohammadi, D., & Cheng, C. S. (1995). A distribution short circuit anlaysis approach using hybrid compensation method. *IEEE Transactions on Power Systems*, *10*(4), 2053–2059.

Zhu, Y., & Tomosovic, K. (2002). Adaptive power flow for distribution systems with dispersed generation. *IEEE Transactions on Power Delivery*, *17*(3), 822–827.